Optimal design method of a wheel travel system for special purpose and robotic vehicle operating over sloped weak sandy terrain

Tatsuro MURO* and Takahisa SHIGEMATSU*

* Civil and Environmental Engineering, Faculty of Engineering, Ehime University 790-77 Japan, E-mail muro@coe.ehime-u.ac.jp

Abstract

In this paper, a mathematical model of vehicle tractive performance was developed and various center of gravity and height of application force movement effects were analysed by mathematical simulation. For given set of vehicle dimensions and terrain-wheel system constants, the simulation calculated, effective tractive effort and rear wheel sinkage, slip ratio of a special designed wheeled robotic vehicle running over sloped weak sandy terrain for straight forward motion. For a 5.88 kN weight vehicle, it is clarified that the optimal eccentricity of center of gravity and the optimal application height are determined as 1/6 and 35 cm respectively, for the range of slope angle less than π/18 rad during driving state of the rear wheel etc..

1: Introduction

This paper addresses the general problem of the design of wheel-base travel systems for special purpose vehicle and robotic machines that are required to move over weak surface or over light bonded terrain of a sandy soil. In relation to the special case of a vehicle travelling on a weak sloped sandy terrain under construction, the paper presents detailed studies of the tractive performance of rear-wheel drive system vehicle with an alternative eccentricity of center of gravity and applcation height configulations. For these studies, a detailed simulation-analytic method was used. Some possibilities for the real time optimal control of the tractive performance of automated and robotic vehicle are outlined.

The objective of this paper is to establish the control system of the position of the eccentricity of center of gravity and the application height of the tractive effort to optimize the tractive performance of a wheeled vehicle. This offers the possibility of dynamically varying these parameters during vehicle travel to maximize traction effort for straight forward motion.

Here, the mechanism of the tractive performance of a 5.88 kN weight, two-axle, four-wheel vehicle with rear-wheel drive system moving up during driving action a sloped terrain of an air-dried decomposed granite soil is considered mathematically. The tractive performance of the wheeled vehicle constructed by two front wheels during unpowered rolling state and two rear wheels during driving action is simulated for a given set of dimension of the vehicle and terrain-wheel system constants. The relationship among the effective tractive effort of the vehicle, the effective driving force of the rear wheel, the amount of sinkage of the front and rear wheel, and the slip ratio of the rear wheel is analysed by use of the simulation-analytic program.

Based on the simulation analytical results, the optimal eccentricity of center of gravity and the optimal application height to obtain the largest effective tractive effort of the vehicle can be determined. Then the effect of the slope angle on the optimal eccentricity of center of gravity and the optimal application height is investigated.

Finally, several automatic control systems to maintain these optimal positions of the eccentricity and the application height for various slope angles are presented.

2: Simulation analysis

The simulation of the tractive or braking performance of a driven or towed rigid wheel on a weak ground was already verified experimentally by use of a rigid wheel of 16 cm radius and 9.5 cm width running on a loose air-dried sandy soil respectively [1] [2]. Here, the tractive performance of the two-axle, four wheel vehicle with rear wheel drive system moving up a sloped terrain of a loose air-dried decomposed granite terrain is considered as the combination of the effective braking force in the unpowered rolling state of the front wheel and the effective driving force during driving action of the rear wheel.

Figure 1 shows the vehicle dimensions and several forces acting on the rear-wheel drive vehicle moving up

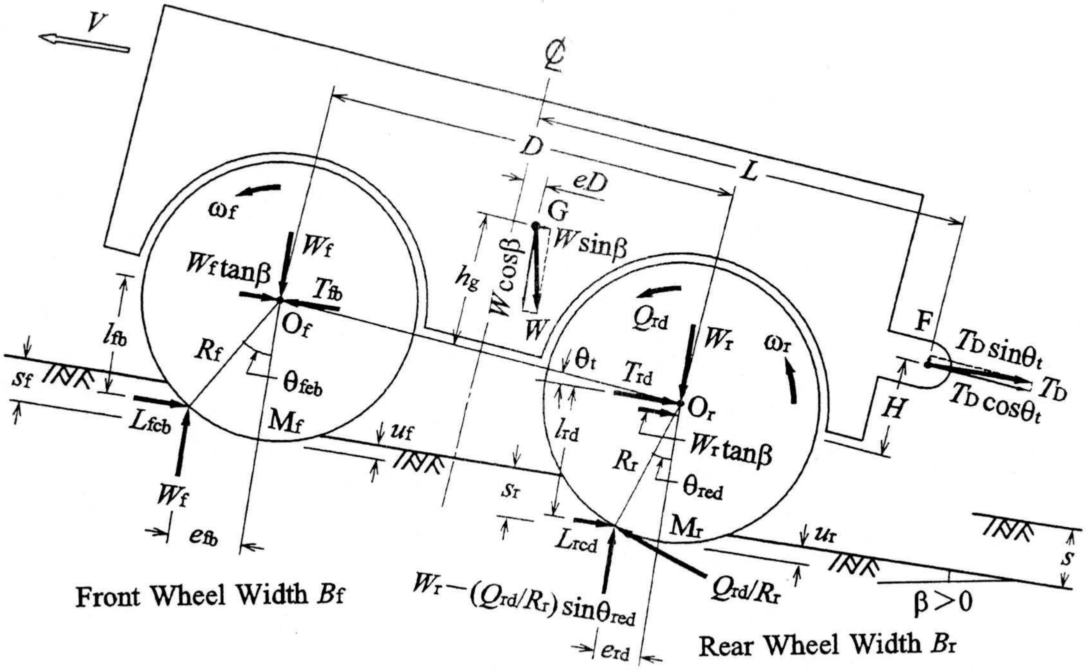

Figure 1 Several forces acting on rear-wheel drive vehicle running up weak terrain of slope angle β

the sloped terrain of angle β during driving action. The vehicle weight W acts vertically on the center of gravity G of the wheeled vehicle, and it is divided into the normal component $W\cos\beta$ and the tangential component $W\sin\beta$ to the sloped terrain. $W\sin\beta$ is called as a slope resistance due to the vehicle weight. The front axle load W_f and the rear axle load W_r act normally to the terrain surface, and the slope resistance $W_f\tan\beta$ and $W_r\tan\beta$ act in parallel to the terrain surface, on the front axle O_f and the rear axle O_r respectively. The position of the center of gravity G is located on the height h_g perpendicular to the line $\overline{O_f O_r}$ and on the amount of eccentricity eD (e is called as an eccentricity of center of gravity of vehicle) from the central axis of the vehicle. D is the wheel base from the front wheel axle to the rear one. R_f and R_r is the radius of front and rear wheel and B_f and B_r is the width of front and rear wheel respectively. The driving torque Q_{dr} acts around the rear axle O_r. The application point F of the effective tractive effort T_D is located on the distance L from the central axis of the vehicle and on the application height H from the line $\overline{O_f O_r}$. During driving action of the rear wheel, the effective braking force T_{bf} in unpowered rolling state is defined to act on the front axle O_f in parallel to the terrain surface, and the effective driving force T_{dr} is defined to act on the rear axle O_r in parallel to the terrain surface, as shown in Fig.1. The vehicle inclined angle θ_t is calculated as the angle between the line $\overline{O_f O_r}$ and the terrain surface.

During driving action of the rear wheel, the unpowered rolling resistance i.e. the compaction resistance L_{fcb} in parallel to the terrain surface and the normal ground reaction W_f are defined to act on the forward contact part of the front wheel at the distance of amount of eccentricity $e_{fb}=R_f\sin\theta_{feb}$ and $l_{fb}=R_f\cos\theta_{feb}$ and the compaction resistance L_{red} in parallel to the terrain surface, the tangential driving force Q_{rd}/R_r, and the normal ground reaction $W_r-Q_{rd}\sin\theta_{red}/R_r$ are defined to act on the forward contact part of the rear wheel at the distance of amount of eccentricity $e_{rd}=R_r\sin\theta_{red}$ and $l_{rd}=R_r\cos\theta_{red}$ as shown in Fig.1.

For the vehicle speed V, the angular velocity ω_f and ω_r of the front and rear wheel, the skid i_{fb} of the front wheel and the slip ratio i_{rd} of the rear wheel are expressed as follows:

$$i_{fb} = \frac{R_f\omega_f}{V} - 1 \tag{1}$$

$$i_{rd} = 1 - \frac{V}{R_r\omega_r} \tag{2}$$

From the force equilibrium in parallel and normal direction to the terrain surface,

$$T_{rd} = \frac{Q_{rd}}{R_r}\cos\theta_{red} - L_{rcd} - W_r\tan\beta \tag{3}$$

$$T_{fb} = -L_{fcb} - W_f\tan\beta \tag{4}$$

$$T_D = T_{rd} + T_{fb}$$

$$= \frac{Q_{rd}}{R_r}\cos\theta_{red} - L_{rcd} - L_{fcb} - W\sin\beta \tag{5}$$

$$W\cos\beta = W_f + W_r \tag{6}$$

are obtained.

From the moment equilibrium around the rear axle O_r,

$$W_f D\cos\theta_t + L_{fcb} D\sin\theta_t - W\cos\beta\{\frac{D}{2} - (eD + h_g\tan\theta_t)\}\cos\theta_t + HT_D\cos\theta_t - (L - \frac{D}{2})T_D\sin\theta_t + W\sin\beta[\frac{h_g}{\cos\theta_t} + \{\frac{D}{2} - (eD + h_g\tan\theta_t)\}\sin\theta_t] = 0 \quad (7)$$

is obtained.

During driving action of the rear wheel, the amount of slippage $j_{dr}(\theta)$ at an arbitrary point of central angle θ is calculated for the entry angle θ_{rf} as follows:

$$j_{dr}(\theta) = R_r\{(\theta_{rf} - \theta) - (1 - i_{rd})(\sin\theta_{rf} - \sin\theta)\} \quad (8)$$

The shear resistance $\tau_r(\theta)$ acting along the circumferential contact part of the rear wheel can be calculated as,

$$\tau_r(\theta) = \{m_c + m_f\sigma_r(\theta)\}[1 - \exp\{-a j_{dr}(\theta)\}] \quad (9)$$

where $\sigma_r(\theta)$ is the normal contact pressure.

Then, the torque Q_{rd} is given as follows:

$$Q_{rd} = 2B_r R_r^2 \int_{-\theta_{rr}}^{\theta_{rf}} \tau_r(\theta)\, d\theta \quad (10)$$

During braking action of the front wheel, the amount of slippage $j_{bf}(\theta)$ at an arbitrary point of central angle θ is calculated for the entry angle θ_{ff} as follows:

$$j_{bf}(\theta) = R_f\{(\theta_{ff} - \theta) - \frac{1}{1 + i_{fb}}(\sin\theta_{ff} - \sin\theta)\} \quad (11)$$

The shear resistance $\tau_f(\theta)$ acting along the circumferential contact part of the front wheel can be calculated as, in the case of $\cos\theta_f - 1 \leqq i_{fb} < 0$;

when traction at $0 \leqq j_{bf}(\theta) \leqq j_p$;

$$\tau_f(\theta) = \{m_c + m_f\sigma_f(\theta)\}[1 - \exp\{-a j_{bf}(\theta)\}] \quad (12)$$

when untraction at $j_q < j_{bf}(\theta) < j_p$;

$$\tau_f(\theta) = \tau_p - k_0\{j_p - j_{bf}(\theta)\}^{n_0} \quad (13)$$

where τ_p, j_p is the shear resistance of soil and the amount of slippage respectively at the beginning of the unloading state.

when reciprocal traction at $j_{bf}(\theta) \leqq j_q$;

$$\tau_f(\theta) = -\{m_c + m_f\sigma_f(\theta)\} \times [1 - \exp[-a\{j_q - j_{bf}(\theta)\}]] \quad (14)$$

Table 1 Terrain-wheel system constants

Front wheel	Rear wheel
k_c = 85.9 N/cm^{n+1}	k_c = 87.3 N/cm^{n+1}
k_ϕ = 9.85 N/cm^{n+2}	k_ϕ = 9.89 N/cm^{n+2}
n = 0.554	n = 0.551
k_{cr} = 180 N/cm^{nr+1}	k_{cr} = 179 N/cm^{nr+1}
$k_{\phi r}$ = 49.3 N/cm^{nr+2}	$k_{\phi r}$ = 49.6 N/cm^{nr+2}
n_r = 0.174	n_r = 0.174
λ = 0.4	λ = 0.4
κ = 1.6	κ = 1.6
k_0 = 2.08 N/cm^{n0+2}	
n_0 = 1.04	
V_0 = 0.035 cm/s	V_0 = 0.035 cm/s
m_c = 0 kPa	m_c = 0 kPa
m_f = 0.434	m_f = 0.434
a = 2.66 1/cm	a = 2.68 1/cm
c_0 = 3.58×10^{-3}	c_0 = 3.51×10^{-3}
c_1 = 0.773	c_1 = 0.772
c_2 = 1.446	c_2 = 1.443

where j_q is the amount of slippage at the beginning of the reverse reloading state.

In the case of $i_{fb} < \cos\theta_f - 1$;

$$\tau_f(\theta) = -\{m_c + m_f\sigma_f(\theta)\}[1 - \exp\{-a j_{bf}(\theta)\}] \quad (15)$$

is obtained.

Then, the torque Q_{fb} is given as follows:

$$Q_{fb} = 2B_f R_f^2 \int_{-\theta_{fr}}^{\theta_{ff}} \tau_f(\theta)\, d\theta \quad (16)$$

For the unpowered rolling state of the front wheel, the skid i_{f0} should be determined by means of the numerical program which calculates repeatedly until the braking torque Q_{fb} becomes zero.

The compaction resistance L_{fcb} and L_{rcd} of the front and rear wheel can be calculated as follows:

$$L_{fcb} = 2(\frac{k_c}{B_f} + k_\phi)\xi B_f \int_0^{s_f} z^n\, dz \quad (17)$$

and

$$L_{rcd} = 2(\frac{k_c}{B_r} + k_\phi)\xi B_r \int_0^{s_r} z^n\, dz \quad (18)$$

$$\xi = \frac{1 + \lambda V_p^\kappa}{1 + \lambda V_0^\kappa}$$

The effective tractive effort T_D can be calculated from the compaction resistance L_{fcb}, the effective driving

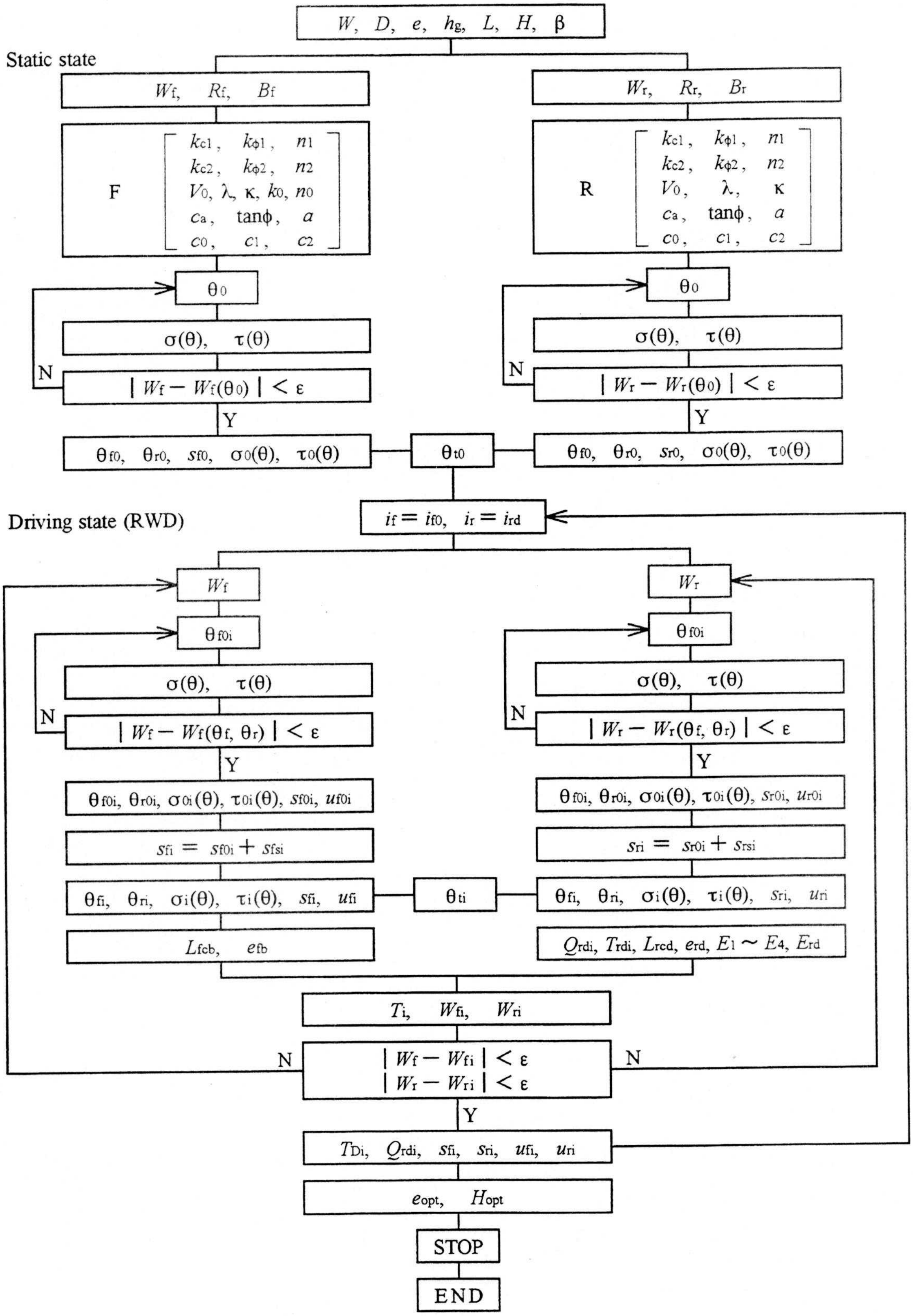

Figure 2 Flow chart for simulation analysis of RWD

Table 2 Vehicle dimensions of two-axle, four-wheel vehicle

Vehicle weight	W	5.88 kN
Radius of front wheel	R_f	15 cm
Radius of rear wheel	R_r	15 cm
Width of front wheel	B_f	10 cm
Width of rear wheel	B_r	10 cm
Eccentricity of center of gravity G	e	$-0.30 \sim 0.30$
Height of center of gravity G	h_g	20 cm
Distance between central axis of vehicle and point F acting effective tractive or braking effort T	L	50 cm
Height of application of effective tractive or braking effort T	H	$0 \sim 60$ cm
Peripheral speed of rear wheel	$R_r \omega_r$	7.07 cm/s
Wheel base from front to rear wheel axle	D	50 cm
Line pressure of front wheel	$W/4B_f$	14.7 kN/m
Line pressure of rear wheel	$W/4B_r$	14.7 kN/m

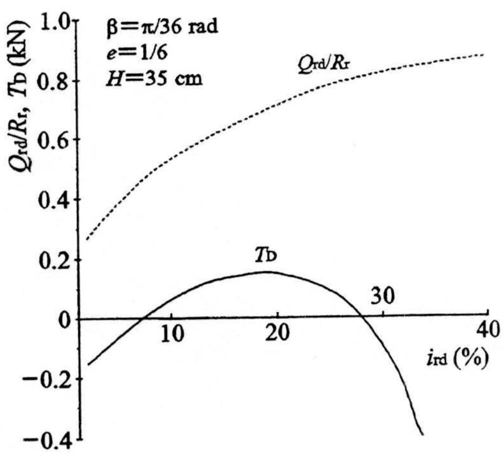

Figure 3 Relationship among driving force Q_{rd}/R_r, effective tractive effort T_D and slip ratio i_{rd} of rear wheel

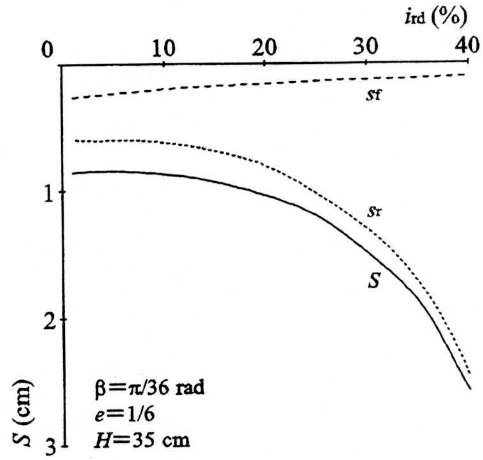

Figure 4 Relationship among amounts of sinkage s_f of front wheel, s_r of rear wheel, S of vehicle and slip ratio i_{rd} of rear wheel

force T_{rd} and the slope resistance. The relationship among T_D and i_{rd}, T_{rd} and i_{rd}, the relationship between Q_{rd} and i_{rd} and the relationship between s_f, s_r and i_{rd} are determined by means of the analytical simulation program, of which flow chart is shown in **Figure 2**.

The tractive performances of the two-axle, four wheel vehicle with rear-wheel drive system were simulated by use of the terrain-wheel system constants [3] given in **Table 1** and the vehicle dimension and the specification given in **Table 2**. To measure the terrain-wheel system constants, an air-dried decomposed granite soil of grain-size adjusted below 4.75 mm and dry density 1.60 g/cm^3, and a smooth steel plate of size 5×10 cm^2 and 10×10 cm^2 was used. The cone index of this sandy terrain measured by means of cone penetrometer test, of which height was 5.0 cm, the apex angle was $\pi/6$ rad and the base area was 6.61 cm^2, was 430 kPa.

As an example, the relationship among the driving force Q_{rd}/R_r of the rear wheel, the effective tractive effort T_D of the vehicle running on the terrain of slope angle $\beta=\pi/36$ rad at the height of application force $H=$ 35 cm and the slip ratio i_{rd} of the rear wheel is shown in **Figure 3**. Q_{rd}/R_r is always larger than T_D for the whole range of slip ratio i. **Figure 4** shows the relationship among the amount of sinkage s_f of the front wheel, s_r of the rear wheel, s of the vehicle and the slip ratio i_{rd} of the rear wheel. s_r and s increase with i_{rd}, while s_f remains almost constant due to the unpowered rolling state.

3: Eccentricity of center of gravity control system

The effect of the position of the center of gravity of the vehicle $e\,D$ on the effective tractive effort T_D can be

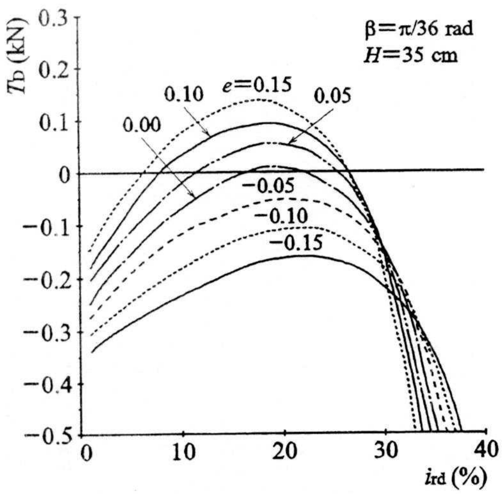

Figure 5 Relationship between effective tractive effort T_D and slip ratio i_{rd} for various kinds of eccentricity e

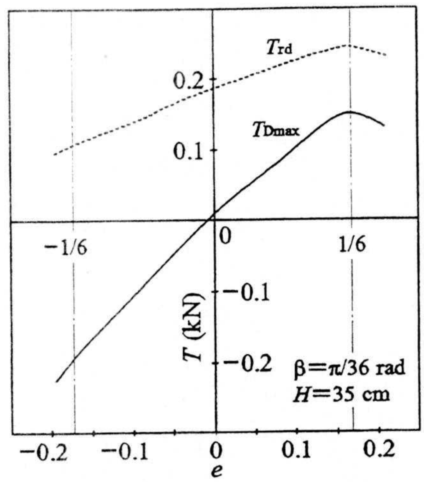

Figure 6 Relationship among maximum effective tractive effort T_{Dmax}, effective driving force T_{rd} and eccentricity e

analysed when the two-axle, four wheel vehicle with rear-wheel drive system is operating during driving action on the weak sandy sloped terrain to pull up other construction machinery. The optimum eccentricity of the center of gravity e_{opt} was defined as the eccentricity to obtain the largest value of the maximum effective tractive effort T_{Dmax}. Here, the value of e_{opt} should be determined within $-1/6 \leqq e_{opt} \leqq 1/6$ because of the safety during operation of the vehicle. That is, the wheeled vehicle becomes to be a dangerous running state due to the negative axle load offront or rear wheel when the resultant force of the vehicle weight and the effective tractive effort applies on the outside range of the middle third of the wheel base.

Figure 5 shows the relationship between the effective tractive effort T_D and the slip ratio i_{rd} of rear wheel for the eccentricity $e=-0.15\sim0.15$ for $\beta=\pi/36$ rad and $H=35$ cm. As shown in this figure, the maximum value of the effective tractive effort T_{Dmax} increases with the increment of eccentricity e. Only in the case of $e \geqq 0.00$, the effective tractive effort shows positive values, and in the case of another eccentricity, the vehicle has to be pushed because of the negative effective effort. **Figure 6** shows the relationship among the maximum effective tractive effort T_{Dmax}, the corresponding effective driving force T_{rd} of rear wheel and the eccentricity e of the center of gravity of the vehicle. T_{Dmax} increases remarkably with the increase of e while T_{rd} increases gradually with e. When T_{Dmax} shows negative values, the vehicle drops down to be unable to pull any more.

T_{Dmax} takes a largest value 0.145 kN at $e=1/6$. In these cases, the skid i_{f0} of the front wheel in unpowered rolling state is maintained from −5.2 % to −7.5 %. So, it is clarified that the optimal eccentricity is determined as $e_{opt}=1/6$ for this rear-wheel drive vehicle moving up the weak terrain of slope angle $\beta=\pi/36$ rad.

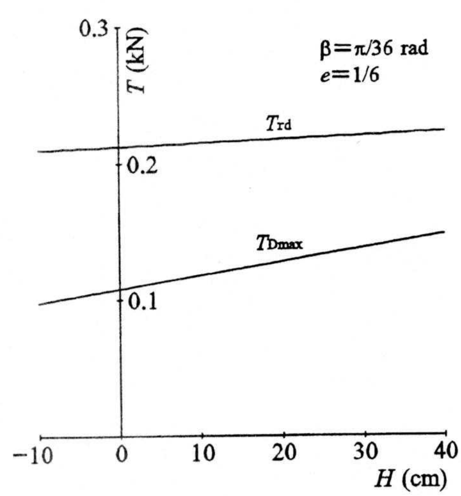

Figure 7 Relationship among maximum effective tractive effort T_{Dmax}, effective driving force T_{rd} and application height H

4: Height of application force control system

The effect of the height of application force H on the effective tractive effort T_D can be analysed when the two-axle, four wheel vehicle with rear-wheel drive system is operating during driving action on the weak sandy sloped terrain to pull up other construction machinery. The optimal application height H_{opt} was defined as the height of application force to obtain the largest value of the maximum effective tractive effort within $0 \leqq H \leqq 35$ cm, considering the vehicle

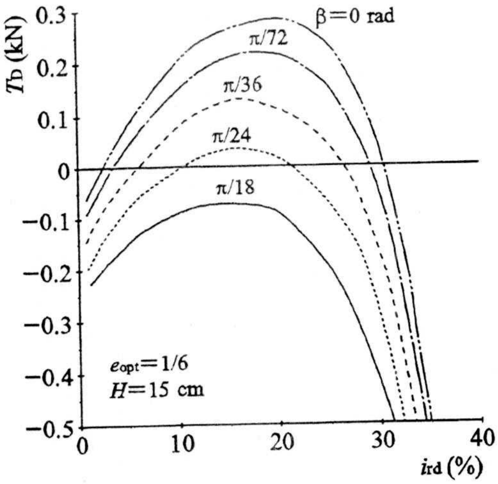

Figure 8 Relationship between effective tractive effort T_D and slip ratio i_{rd} for various slope angles β

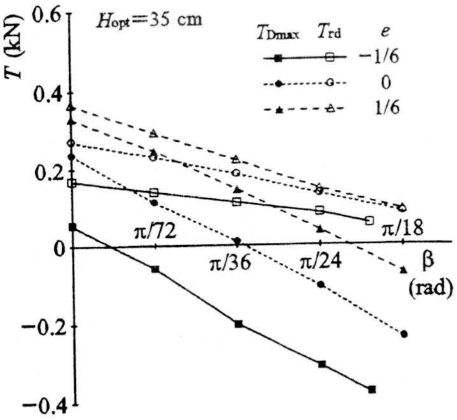

Figure 9 Relationship among maximum effective tractive effort T_{Dmax}, effective driving force T_{rd} and slope angle β for three kinds of eccentricity e

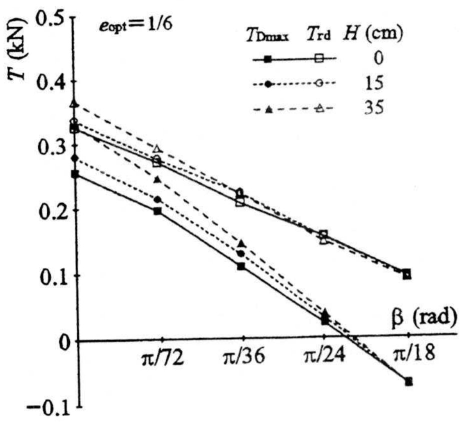

Figure 10 Relationship among maximum effective tractive effort T_{Dmax}, effective driving force T_{rd} and slope angle β for three kinds of application height H

specification of the clearance and the hook position to pull other construction machinery.

Figure 7 shows the relationship among the maximum effective tractive effort T_{Dmax} of the rear-wheel drive vehicle, the corresponding effective driving force T_{rd} of the rear wheel and the application height H of the effective tractive effort. These simulation results are obtained for the slope angle $\beta=\pi/36$ rad and the eccentricity $e=1/6$. As a result, the largest value of the maximum effective tractive effort $T_{Dmax}=0.145$ kN is obtained at $H=35$ cm. So, it is clarified that the optimal application height is determined as $H_{opt}=35$ cm for this rear-wheel drive vehicle moving up the weak terrain of slope angle $\beta=\pi/36$ rad.

5: Effect of slope angle

The effects of the slope angle β of the terrain on the effective tractive effort T_D can be analysed when the two-axle, four wheel and rear-wheel drive system are operating during driving action on the weak sandy sloped terrain to pull up other construction machinery.

Figure 8 shows the relationship between the effective tractive effort T_D of the vehicle and slip ratio i_{rd} of the rear wheel for various slope angles β when the two-axle, four wheel and rear-wheel drive vehicle is operating at some condition of $e_{opt}=1/6$ and $H=15$ cm. T_D increases with the increase of i_{rd} , but it decreases remarkably with i_{rd} due to the increasing amount of slip sinkage of the rear wheel and the increasing positive slope resistance $W\sin\beta$ after taking the maximum value T_{Dmax} at about $i_{rd}=15\sim20$ %. The maximum effective tractive effort T_{Dmax} decreases with the increase of the slope angle.

Figure 9 shows the relationship among the maximum effective tractive effort T_{Dmax}, the corresponding effective driving force T_{rd} and the slope angle β of the terrain for the eccentricity $e=-1/6$, 0 and 1/6 when the two-axle, four wheel and rear-wheel drive vehicle is moving up the weak sandy sloped terrain at $H_{opt}=35$ cm. The maximum effective tractive effort T_{Dmax}, the effective driving force T_{rd} decrease remarkably with the increment of the slope angle β. The difference between T_{rd} and T_{Dmax} becomes large with the increment of β due to the increasing slope resistance. In this case, it is clarified that the maximum slope angle of the terrain β_{max} to pull up other construction machinery is about 0.146 rad when the vehicle is operating at $e=1/6$ and $H_{opt}=35$ cm, and T_{Dmax} shows a larger value for each slope angle when the amount of eccentricity of the center of gravity moves to the rear part.

Figure 10 shows the relationship among the maximum effective tractive effort T_{Dmax}, the corresponding effective driving force T_{rd} and the slope angle β of the terrain for the application height $H=0$, 15, 35 cm when the two-axle, four wheel and rear-wheel drive vehicle is moving up the weak sandy sloped terrain at $e_{opt}=1/6$. The maximum effective tractive effort T_{Dmax}, the effective driving force T_{rd} decrease remarkably with the increment of the slope angle β. The difference between T_{rd} and T_{Dmax} becomes large with the increment of β due to the increasing slope resistance. In this case, it is also clarified that the maximum slope angle of the terrain β_{max} to pull up other construction machinery is about 0.146 rad when the vehicle is operatingat $e=1/6$ and $H_{opt}=35$ cm, and T_{Dmax} shows a larger value for each slope angle when the position of the application height moves upward.

6: Conclusion

The maximum effective tractive effort of a two-axle, four wheel, rear-wheel drive vehicle moving up a weak sandy sloped terrain vary with the position of the center of gravity and the application height of the effective tractive effort, respectively. So, the tractive performance of a 5.88 kN weight, rear-wheel drive vehicle was simulated by use of the terrain-wheel system constants. Especially, the optimal eccentricity of the center of gravity and the optimal application height of the effective tractive effort should be determined for the terrain of various slope angles to obtain the largest value of the maximum effective tractive effort.

Several new analytical results are summarized as follows:

(1) During driving state of the rear wheel, the optimal eccentricity of the center of gravity e_{opt} is determined as 1/6 for the range of slope angle $0 \leqq \beta \leqq \pi/18$ rad.
(2) During driving state of the rear wheel, the optimal application height H_{opt} is determined as 35 cm for the range of slope angle $0 \leqq \beta \leqq \pi/18$ rad.
(3) The maximum slope angle of the terrain to pull up other construction machinery is about 0.146 rad when the vehicle is operating at $e_{opt}=1/6$ and $H_{opt}=35$ cm, and the maximum effective tractive effort shows a larger value for each slope angle when the amount of eccentricity of the center of gravity moves to the rear part of the vehicle and the position of the application height moves upward.
(4) From these simulation results, the automatic control system for the optimal eccentricity of the center of gravity and the optimal application height can be expected by use of some clinometer sensor mounted on the vehicle.

References

[1] T.Muro : Braking performance of a towed rigid wheel on a soft ground based on the analysis of soil compaction, Soils and Foundations, 33(2), pp.91-104, 1993.
[2] T.Muro : Tractive performance of a driven rigid wheel on soft ground based on the analysis of soil-wheel interaction, Journal of Terramechanics, 30(5), pp.351-369, 1993.
[3] T.Muro, Y.Hoshika and S.Kawahara : Optimum trafficability control system of a two-axle, two-wheel road roller during driving and braking action, Journal of Construction Management and Engineering, JSCE, No.534/VI-30, pp.201-212, March, 1996. (In Japanese)